Radiation-Perturbed Flow Fields of Normal and Oblique Shock Waves

D. B. Olfe*
New York University, Bronx, N. Y.

Flow field perturbations due to radiative transfer behind normal and oblique shock waves are studied. For steady, two-dimensional flow, the perturbation equations of motion reduce to Poisson and wave equations for subsonic and supersonic flow, respectively, with source terms determined by the radiative transfer. Consideration of boundary conditions yields general solutions, which can include the effects of absorption ahead of the shock and external radiation sources such as emitting or reflecting boundaries. For a normal shock with radiant-energy transfer parallel to the shock front, the perturbed flow variables and shock curvature are determined. Introduction of an approximation for the radiative transfer term in the oblique shock (supersonic wedge) case, yields explicit solutions for the perturbed flow variables and shock curvature. These analyses are valid for either frozen or equilibrium flow, and the effects of self-absorption are included, with explicit results being obtained for a gray gas and a gas with nonoverlapping spectral lines described by collision-broadened profiles.

I. Introduction

PRESENT-DAY problems in aeronautics and astronautics, such as high-velocity re-entry, have recently produced a widespread interest in the subject of radiation gasdynamics. The addition of radiation to gasdynamics results in a vast increase in the complexities of the problems, so that solutions are usually obtained by considering limiting forms of the radiative transfer (transparent and diffusion gas limits), or by considering the radiation to act as a perturbation. The latter approach is used in this paper because, in the perturbation treatment, the radiation term can retain a general form, and because, in aeronautics problems such as re-entry, the radiation is now only approaching a magnitude great enough to become important in determining the flow field.

In this paper, the equations satisfied by the perturbation flow variables and the relations at the shock front are first determined, with the shock front assumed to be transparent, although the gas ahead and behind the shock may be self-absorbing. The problems of the normal and oblique shock-wave flow fields are then treated separately. The oblique shock flow (supersonic wedge) is solved by transformation to the corresponding one-dimensional unsteady normal shock flow, considered in Ref. 1. In the transparent gas limit, the solutions agree with those of Ref. 2 where solutions were obtained only for the transparent gas regime.

Although this paper does not include calculations for particular re-entry trajectories, it appears worthwhile to briefly discuss the re-entry application. A number of studies on the effect of radiative transfer on the shock layer near the stagnation region of a blunt body have been carried out during the past few years (see, e.g., Goulard,[3] Kennet,[4] Yoshikawa and Chapman,[5] Howe and Viegas,[6] and Wilson and Hoshizaki[7]). These studies show that radiant-energy transfer can appreciably affect the flow fields of blunt bodies traveling at very high re-entry velocities, corresponding to near the parabolic velocity or greater. Although the wedge will distribute the flow energy more evenly, resulting in lower radiative transfer than for the corresponding blunt-body case, the radiation can affect the flow field about a wedge for very high speed flows. For example, Zhigulev et al.[2] calculate appreciable perturbations in the flow field of a wedge of 35° half angle traveling at $M_\infty = 60$ at 60 km-alt. The blunt-body studies were carried out for transparent and gray gases, with the gray gas analyses showing that self-absorption can become important in certain cases. The larger shock-layer thickness near the base of a wedge and deeper atmospheric penetration before peak heating indicate that self-absorption may be more important for wedge flow than for the stagnation region of a blunt body. None of the papers known to this author have treated self-absorbed spectral line radiation, which can be an important contributor to the total radiant-energy flux.

II. Perturbation Equations of Motion

In this analysis we consider shock-wave flow fields that would have constant values for the flow variables ahead and behind the shock fronts in the absence of radiation. Our treatment accounts for chemical reactions (including dissociation, ionization, electronic excitation, etc.). However, the requirement of constant flow variables in the radiationless problem restricts us to either frozen or equilibrium flow.

The perturbed equations of motion are obtained by expressing each flow variable as the sum of the constant value for the nonradiating gas and the perturbation quantity, e.g., $\tilde{\rho} = \rho_0 + \rho$, where ρ_0 is the density in the radiationless case and ρ is the change in density caused by radiation. Choosing coordinate systems ahead and behind the shock such that the y component of the gas velocity is zero in the radiationless case, the perturbed equations of motion are

$$\rho_0 \frac{\partial u}{\partial x} + \rho_0 \frac{\partial v}{\partial y} + U_0 \frac{\partial \rho}{\partial x} = 0 \tag{1}$$

$$\rho_0 U_0 \frac{\partial u}{\partial x} = -\frac{\partial p}{\partial x} \tag{2}$$

$$\rho_0 U_0 \frac{\partial v}{\partial x} = -\frac{\partial p}{\partial y} \tag{3}$$

$$U_0 \frac{\partial E}{\partial x} + \frac{p_0}{\rho_0}\left(\frac{\partial u}{\partial x} + \frac{\partial v}{\partial y}\right) + e_0 = 0 \tag{4}$$

Presented as Preprint 64-69 at the AIAA Aerospace Sciences Meeting, New York, January 20–22, 1964; revision received May 20, 1964. The research reported in this paper was sponsored by the National Science Foundation under Grant NSF-GP-562.

* Associate Professor of Aeronautics; now Associate Professor of Aerospace Engineering, University of California at San Diego, La Jolla, Calif. Member AIAA.

where E is the perturbed internal energy per unit mass. The quantity e_0 is the net rate of radiant energy emission per unit mass (energy emitted minus the energy absorbed), which is computed using the unperturbed quantities $e_0 = e_0\{T_0, p_0; x, y\}$. In Secs. IV and V, e_0 will be computed for particular cases by using the relation $e_0 = \nabla \cdot \mathbf{F}/\rho_0$ where $\mathbf{F}$ is the radiation flux. Here the general form e_0 will be retained so that the effects of self-absorption, external radiation, etc., are implicitly included. In the preceding equations, radiative transfer enters in only as an energy loss term in the energy equation, since we have neglected the radiation pressure and energy density terms (valid for most applications).

In order to retain the effects of chemical reaction for equilibrium flows, the perturbed and unperturbed equations of state are given by

$$\frac{T}{T_0} = h\frac{p}{p_0} - k\frac{\rho}{\rho_0} \tag{5}$$

$$p_0 = z\rho_0 R T_0 \tag{6}$$

whereas the perturbation of internal energy is given by

$$E = fRT - g(RT_0/p_0)p \tag{7}$$

where R is the gas constant for the pure gas. The quantities h, k, z, f, and g are functions of T_0 and p_0, and have forms that depend on the particular reactions taking place. For a perfect gas, $h = k = z = 1$, $g = 0$, and $f = (\gamma - 1)^{-1}$ where γ is the ratio of specific heats. For an ionizing monatomic gas in equilibrium, the ionization (Saha) equation may be utilized to obtain the following results:

$$h = \left[1 + \frac{\tilde{\alpha}_0}{2}(1 - \tilde{\alpha}_0)\right] \Big/ \left[1 + \frac{\tilde{\alpha}_0}{2}(1 - \tilde{\alpha}_0)\left(\frac{5}{2} + \frac{T_{\text{ion}}}{T_0}\right)\right]$$

$$k = \left[1 + \frac{\tilde{\alpha}_0}{2}(1 - \tilde{\alpha}_0)\left(\frac{5}{2} + \frac{T_{\text{ion}}}{T_0}\right)\right]^{-1}$$

$$g = \frac{\tilde{\alpha}_0}{2}(1 - \tilde{\alpha}_0^2)\left(\frac{3}{2} + \frac{T_{\text{ion}}}{T_0}\right)$$

$$z = (1 + \tilde{\alpha}_0)$$

$$f = \left[\frac{3}{2}(1 + \tilde{\alpha}_0) + \frac{\tilde{\alpha}_0}{2}(1 - \tilde{\alpha}_0^2)\left(\frac{5}{2} + \frac{T_{\text{ion}}}{T_0}\right)\left(\frac{3}{2} + \frac{T_{\text{ion}}}{T_0}\right)\right]$$

where $\tilde{\alpha}_0$ is the degree of ionization (mass fraction of atoms ionized) in the radiationless problem and T_{ion} is the ionization potential divided by the Boltzmann constant.

Equations (1 and 4–7) may be combined to yield

$$U_0\frac{\partial \rho}{\partial x} = \frac{U_0}{a^2}\frac{\partial p}{\partial x} + \rho_0\epsilon \tag{8}$$

where

$$a^2 \equiv \left(\frac{fk + z}{fh - g}\right)\frac{p_0}{\rho_0} \tag{9}$$

$$\epsilon \equiv \left(\frac{1}{fk + z}\right)\left(\frac{e_0}{RT_0}\right) \tag{10}$$

Equation (9) yields a frozen or equilibrium speed of sound, whichever the case may be, whereas the effect of reactions on the radiative transfer term is given by Eq. (10).

For a perfect gas, Eqs. (9) and (10) become

$$a^2 = \frac{\gamma p_0}{\rho_0} \qquad \epsilon = \left(\frac{\gamma - 1}{\gamma}\right)\left(\frac{e_0}{RT_0}\right) = \frac{e_0}{c_p T_0}$$

Fig. 1 Geometry and notation for the oblique shock wave.

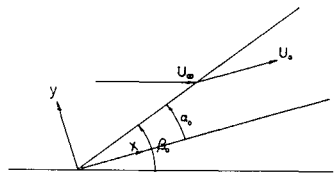

respectively, where c_p is the specific heat at constant pressure.

The following perturbation equations of motion are obtained from Eqs. (1–3 and 8):

$$(M^2 - 1)\frac{\partial^2 p}{\partial x^2} - \frac{\partial^2 p}{\partial y^2} = -\rho_0 U_0\frac{\partial \epsilon}{\partial x} \tag{11}$$

$$(M^2 - 1)\frac{\partial^2 v}{\partial x^2} - \frac{\partial^2 v}{\partial y^2} = \frac{\partial \epsilon}{\partial y} \tag{12}$$

where $M \equiv U_0/a$. For $M > 1$, these equations are wave equations with source terms $-\rho_0 U_0 \partial\epsilon/\partial x$ and $\partial\epsilon/\partial y$ determined by the radiation from the unperturbed flow. Poisson's equation results when $M < 1$.

An alternative way of expressing the equations satisfied by the perturbation quantities is to define a potential φ by

$$p = -\rho_0 U_0(\partial\varphi/\partial x) \qquad v = \partial\varphi/\partial y \tag{13}$$

Combining Eqs. (1–3 and 8) yields the following equation satisfied by φ:

$$(M^2 - 1)(\partial^2\varphi/\partial x^2) - (\partial^2\varphi/\partial y^2) = \epsilon \tag{14}$$

The boundary conditions on p and v become conditions on $\partial\varphi/\partial x$ and $\partial\varphi/\partial y$, respectively.

III. Relations between the Perturbed Quantities at the Shock Front

Assuming that radiative transfer is unimportant within the gasdynamic shock thickness, the following relations between the perturbed variables hold at an oblique shock front (see Fig. 1):

$$\alpha = \Psi(v_s/U_0) + A \tag{15a}$$

$$p_s/p_0 = \Gamma(v_s/U_0) + B \tag{15b}$$

$$\rho_s/\rho_0 = \Delta(v_s/U_0) + C \tag{15c}$$

$$u_s/U_0 = \Omega(v_s/U_0) + D \tag{15d}$$

where α is the perturbation of the angle α_0 between the wedge surface and the shock front.

If absorption or emission of radiation ahead of the shock wave is unimportant, then A, B, C, and D are all zero, which is the case that will be considered in this paper. When radiation ahead of the shock is important, Eqs. (11) and (12) can be solved in the region ahead of the shock, where they are wave equations, to determine the perturbed flow variables as discussed in Ref. 1 and in the manner of solution discussed in Sec. V. The shock relations can then be used to determine A, B, C, and D in terms of the perturbations ahead of the shock. Considering that an actual shock is of finite length, the absorption of radiation from the shocked gas by the gas ahead of the shock will be unimportant when the photon mean free path ahead of the shock is appreciably greater than the shock length, i.e., when little of the absorbed energy passes back through the shock front.

The following expressions for Ω, Ψ, Γ, and Δ are obtained by considering the conservation equations across an oblique shock wave:

$$\Omega = \frac{\left[1 - \frac{1}{2}\left(1 - \frac{\rho_\infty}{\rho_0}\right)\left[1 + \left(\frac{fh - g + z}{fk + z}\right)\frac{\rho_0 U_0^2}{p_0}\sin^2\alpha_0\right]\cot\alpha_0\right.}{1 + \frac{1}{2}\left(\frac{z}{fk + z}\right)\left(\frac{\rho_0 U_0^2}{p_0}\right) - \frac{1}{2}\left(1 + \frac{\rho_\infty}{\rho_0}\cot^2\alpha_0\right)\left[1 + \left(\frac{fh - g + z}{fk + z}\right)\frac{\rho_0 U_0^2}{p_0}\sin^2\alpha_0\right]} \tag{16a}$$

$$\Psi = -\left(\frac{\rho_0}{\rho_\infty} - 1\right)^{-1}(1 + \Omega \cot\alpha_0) \tag{16b}$$

$$\Gamma = -\frac{1}{2}\left(\frac{\rho_0 U_0^2}{p_0}\right)\sin 2\alpha_0\left[\left(\tan\alpha_0 + \frac{\rho_\infty}{\rho_0}\cot\alpha_0\right)\Omega + \left(\frac{\rho_\infty}{\rho_0} - 1\right)\right] \tag{16c}$$

$$\Delta = \left(1 + \frac{\rho_\infty}{\rho_0}\right)\cot\alpha_0 + \left[\frac{\rho_\infty}{\rho_0}\csc^2\alpha_0 - \left(1 + \frac{\rho_\infty}{\rho_0}\right)\right]\Omega \tag{16d}$$

For a normal shock wave the foregoing relations reduce to

$$\Omega = \Gamma = \Delta = 0 \tag{17a}$$

$$\Psi = -[(\rho_0/\rho_\infty) - 1]^{-1} \tag{17b}$$

In Eqs. (16), the quantities h, k, z, g, and f are those appropriate for the gas behind the shock front. For example, if dissociation is complete but ionization not yet important, then these quantities should have the monatomic gas values, $h = k = z = 1, g = 0, f = \frac{3}{2}$. If ionization and/or dissociation is occuring in the shocked gas, then these effects can be explicitly accounted for (see Sec. II), or one can use the perfect gas relations with a value of γ chosen to reflect the real-gas properties. The unperturbed flow field quantities ρ_∞/ρ_0 and $\rho_0 U_0^2/p_0$, which appear in Eqs. (16), depend on the real-gas effects across the shock front. The appropriate value of γ for approximating the real-gas effects across a shock front will generally differ from the value of appropriate for the gas behind the shock front. Even though they are of limited use, it is of interest to look at the perfect gas forms of Eqs. (16):

$$\Omega = \left[\frac{2(\gamma M^4 \sin^4\alpha_0 + 1)\cot\alpha_0}{2\gamma M^4 \sin^4\alpha_0 - (3\gamma - 1)M^4 \sin^2\alpha_0 - (3 - \gamma)M^2 + 2}\right] \tag{18a}$$

$$\Gamma = \frac{-\gamma M^2 \sin\alpha_0 \cos\alpha_0}{(\gamma - 1)M^2 \sin^2\alpha_0 + 2}[(2 + (\gamma + 1)M^2 - 2M^2 \sin^2\alpha_0)\Omega \tan\alpha_0 - 2(1 - M^2 \sin^2\alpha_0)] \tag{18b}$$

$$\Psi = -\left(\frac{\gamma + 1}{2}\right)\left(\frac{M^2 \sin^2\alpha_0}{1 - M^2 \sin^2\alpha_0}\right)(1 + \Omega \cot\alpha_0) \tag{18c}$$

$$\Delta = \frac{2(1 + \gamma M^2 \sin^2\alpha_0)\cot\alpha_0 - [2(1 + \gamma M^2 \sin^2\alpha_0) - (\gamma + 1)M^2]\Omega}{(\gamma - 1)M^2 \sin^2\alpha_0 + 2} \tag{18d}$$

For a given shock-layer angle α_0, the Mach number M behind the shock will decrease from the weak shock limit of $M = \csc\alpha_0$ to the strong shock limit of $M = [(\gamma - 1)/2\gamma]^{1/2}\csc\alpha_0$. For the strong shock limit and $\alpha_0 \ll 1$, Eqs. (18) reduce to

$$\Omega = -\left(\frac{2\gamma}{\gamma - 1}\right)\alpha_0 \qquad \Gamma = (\gamma - 1)\frac{1}{\alpha_0}$$
$$\Psi = \left(\frac{\gamma + 1}{2}\right) \qquad \Delta = 0 \tag{19}$$

For the shock layer of a supersonic wedge, α_0 will be quite small, even for quite large wedge angles.

IV. Perturbed Flow Field of a Normal Shock Wave

General Solution

A shock wave perturbed from the normal direction by an angle $-\alpha\{y\}$ is illustrated in Fig. 2a. If an emitting gas bounded by the two planes $y = \pm h$ is considered, as shown in Fig. 2b, then the boundary condition $v\{y = \pm h\} = 0$ can be satisfied by distributing sources from $y = -\infty$ to $y = +\infty$ with a strength distribution $\epsilon\{x, y\} = \epsilon\{x, y \pm 2nh\}$, where $n = 0, 1, 2, \ldots$ (this distribution also covers the case of an absorbing gas bounded by the planes $y = 0$ and $y = +h$). For the normal shock, Eq. (11) becomes Poisson's equation since $M < 1$. In order to satisfy the relation $p_s/p_0 = B\{y\}$ given by Eqs. (15b) and (17a), radiation sources are placed in the region $x < 0$ with the strength distribution $\epsilon\{x, y\} = \epsilon\{|x|, y\}$, and a line source of strength $\tilde{\sigma}\{y\}$ is placed at the shock front ($x = 0$), with $\tilde{\sigma}$ to be determined by $B\{y\}$.

The solution of Eq. (11) (Poisson's equation) becomes, upon integration by parts,

$$\frac{p}{p_0} = \frac{1}{2\pi}\left(\frac{\rho_0 U_0}{p_0}\right)\frac{1}{(1 - M^2)^{1/2}} \times \left\{\int_{-\infty}^{+\infty}\int_{-\infty}^{+\infty}\frac{\epsilon\{\xi,\eta\}(x - \xi)d\xi d\eta}{[(x - \xi)^2 + (1 - M^2)(y - \eta)^2]} + \int_{-\infty}^{+\infty}\frac{\tilde{\sigma}\{\eta\}x d\eta}{[x^2 + (1 - M^2)(y - \eta)^2]}\right. \tag{20}$$

The condition $p_s = p\{0, y\} = p_0 B\{y\}$ yields

$$\tilde{\sigma}\{y\} = 2(1 - M^2)(p_0/\rho_0 U_0)B\{y\} \tag{21}$$

In the following section, we consider an example for which the effect of radiation ahead of the shock is assumed negligible, so that $B\{y\} = 0$. A study of the interaction of a normal shock with a thermal boundary layer[8] uses the same formula as the preceding but with $\epsilon\{x, y\} = 0$ and $B\{y\}$ proportional to the temperature perturbation just ahead of the shock. The solution of Eq. (12) is

$$\frac{v}{U_0} = -\frac{(1 - M^2)^{1/2}}{2\pi U_0} \times \left\{\int_{-\infty}^{+\infty}\int_{-\infty}^{+\infty}\frac{\epsilon\{\xi, \eta\}(y - \eta)d\xi d\eta}{[(x - \xi)^2 + (1 - M^2)(y - \eta)^2]} + \int_{-\infty}^{+\infty}\frac{\tilde{\sigma}\{\eta\}(y - \eta)d\eta}{[x^2 + (1 - M^2)(y - \eta)^2]}\right\} \tag{22}$$

and use of Eqs. (15a) and (17b) gives the following result:

$$\alpha = \frac{(1 - M^2)^{1/2}}{2\pi U_0[(\rho_0/\rho_\infty) - 1]} \times \left\{\int_{-\infty}^{+\infty}\int_{-\infty}^{+\infty}\frac{\epsilon\{\xi, \eta\}(y - \eta)d\xi d\eta}{[\xi^2 + (1 - M^2)(y - \eta)^2]} + \left(\frac{1}{1 - M^2}\right)\int_{-\infty}^{+\infty}\frac{\tilde{\sigma}\{\eta\}}{(y - \eta)}\right\}d\eta \tag{23}$$

By integration of Eqs. (2) and (8) with the conditions at the shock front given by Eqs. (15c, 15d, and 17a), the following relations for u and ρ are obtained:

$$\frac{u}{U_0} = -\left(\frac{p_0}{\rho_0 U_0^2}\right)\left[\frac{p\{x, y\}}{p_0} - B\{y\}\right] + D\{y\} \tag{24}$$

$$\frac{\rho}{\rho_0} = M^2\left(\frac{p_0}{\rho_0 U_0^2}\right)\left[\frac{p\{x, y\}}{p_0} - B\{y\}\right] + C\{y\} + \frac{1}{U_0}\int_0^x \epsilon\{\xi, y\}d\xi \tag{25}$$

The temperature perturbation can be obtained from Eq. (5).

Example Calculation: Absorption of Radiation Parallel to the Shock Front

For an example calculation, we consider a semi-infinite normal shock wave perturbed by the absorption of uniform parallel radiation from the negative y direction. It is assumed that the radiation is absorbed only by the shocked gas extending a distance L behind the shock front, and that $L \gg (1 - M^2)^{1/2}\, l$ where l is the photon mean free path ($l = 1/\bar{k}$ where $\bar{k}$ is the mean absorption coefficient for the shocked gas). Except within a small distance of order $(1 - M^2)^{1/2}\, l$ of the point $x = L$, $y = 0$, Eq. (20) can be integrated approximately to yield

$$\frac{p}{p_0} \simeq \frac{1}{2\pi}\left(\frac{z}{fk + z}\right)(1 - M^2)^{-1/2}\left(\frac{\rho_0 U_0^2}{p_0}\right)\left(\frac{F_0}{p_0 U_0}\right) \times \ln\left[\frac{(L + x)^2 + (1 - M^2)y^2}{(L - x)^2 + (1 - M^2)y^2}\right] \quad (26)$$

It is seen from this equation that the pressure perturbation depends only on the total radiant energy flux F_0 absorbed, and not on the particular absorbing properties of the gas. The pressure perturbation increases from zero at the shock front to a maximum at $x = L$ and then approaches zero as $x \to \infty$, and also decreases with increasing y.

Equation (22) for the y velocity perturbation can be integrated approximately to yield

$$\frac{v}{U_0} \simeq \frac{1}{\pi}\left(\frac{z}{fk + z}\right)\left(\frac{F\{0\} - F\{y\}}{p_0 U_0}\right) \times \left[\tan^{-1}\left\{\frac{L + x}{(1 - M^2)^{1/2} y}\right\} + \tan^{-1}\left\{\frac{L - X}{(1 - M^2)^{1/2} y}\right\}\right] \quad (27)$$

At small $y (y \lesssim 2l)$, the velocity perturbation depends on the particular absorbing properties of the gas through the term $F\{0\} - F\{y\}$ giving the decrease in radiant-energy flux in the y direction, whereas at large $y (y \gg l)$, the perturbation depends only on the value of L, i.e., only on the x-variation of the flux (these regions are separated because we are considering the case $(1 - M^2)^{1/2} l \ll L$).

Perturbations for the x velocity, density, and temperature are determined from Eqs. (24, 25, and 5), respectively:

$$\frac{u}{U_0} = -\left(\frac{p_0}{\rho_0 U_0^2}\right)\frac{p\{x, y\}}{p_0} \quad (28)$$

$$\frac{\rho}{\rho_0} = M^2\left(\frac{p_0}{\rho_0 U_0^2}\right)\frac{p\{x, y\}}{p_0} + \epsilon\{y\}\cdot\frac{x^*}{U_0} \quad (29)$$

$$\frac{T}{T_0} = \left[h - kM^2\left(\frac{p_0}{\rho_0 U_0^2}\right)\right]\frac{p\{x, y\}}{p_0} - k\epsilon\{y\}\,\frac{x^*}{U_0} \quad (30)$$

where $x^* \equiv x$ for $x < L$ and $x^* \equiv L$ for $x > L$. The density and temperature perturbations depend on the gas absorbing properties through the $\epsilon\{y\}\cdot x^*/U$ term, which is proportional to the rate of absorption at y multiplied by the time over which the gas element has been absorbing radiation.

The shock-angle perturbation is obtained directly from Eqs. (15a, 17b, and 27):

$$\alpha \simeq -\frac{2}{\pi}\left(\frac{\rho_0}{\rho_\infty} - 1\right)^{-1}\left(\frac{z}{fk + z}\right) \times \left(\frac{F\{0\} - F\{y_s\}}{p_0 U_0}\right)\tan^{-1}\left\{\frac{L}{(1 - M^2)^{1/2} y_s}\right\} \quad (31)$$

Gray gas

A gray gas is characterized by a constant (independent of frequency) absorption coefficient $\bar{k}$. Gases for which continuum processes dominate the spectrum may approximate a gray gas, as may a gas with bands consisting of lines that are well overlapped. In the latter case, particularly, the gray-gas absorption may occur in only part of the spectrum, whereas the rest of the spectrum may be considered to be transparent. The flux and absorption terms for a gray gas are

$$F\{0\} - F\{y\} = F_0(1 - e^{-\bar{k}y})$$
$$\epsilon\{y\} = \left(\frac{z}{fk + z}\right)\frac{\bar{k}F_0}{p_0}\,e^{-\bar{k}y} \quad (32)$$

where F_0 is the flux incident in the spectral region where the absorption coefficient is $\bar{k}$. These results can be extended to a number of nonoverlapping gray spectral regions with absorption coefficients $\bar{k}_1, \bar{k}_2, \ldots, \bar{k}_N$ by adding the resulting perturbations for each $\bar{k}_i$ value.

The expressions in Eq. (32) may be substituted into Eqs. (27–31) to obtain the flow field perturbations. Equation (31) for the perturbed shock angle can be integrated to give the following expressions for the shape of the shock front:

$$\left(\frac{2\gamma}{\gamma^2 - 1}\right)\left(\frac{1 - M^2}{M^2}\right)\left(\frac{p_0 U_0}{F_0}\right)\bar{k}x_s = \bar{k}y_s + e^{-\bar{k}y_s} - 1 \quad \text{for } y \ll \frac{L}{(1 - M^2)^{1/2}} \quad (33)$$

$$\left(\frac{2\gamma}{\gamma^2 - 1}\right)\left(\frac{1 - M^2}{M^2}\right)\left(\frac{p_0 U_0}{F_0}\right)\left[(1 - M^2)^{1/2}\frac{x_s}{L}\right] = \frac{2}{\pi}\left[\eta\cot^{-1}\eta + \frac{1}{2}\ln(1 + \eta^2)\right] \quad \text{for } y \gg l \quad (34)$$

where $\eta \equiv (1 - M^2)^{1/2}(y_s/L)$, and we have used the perfect-gas result,

$$\left(\frac{\rho_0}{\rho_\infty} - 1\right)\left(\frac{fk + z}{z}\right) = \left(\frac{2\gamma}{\gamma^2 - 1}\right)\left(\frac{1 - M^2}{M^2}\right)$$

Equation (33) for large $\bar{k}y_s$ reduces to the same expression as Eq. (34) does for small η. These equations are plotted in Fig. 3. The shock front is seen to curve towards the shocked gas from its normal position at $y = 0$, achieving a nearly constant slope at a couple of photon mean free paths ($\bar{k}y_s \simeq 2$), and then it starts to curve back towards the normal position when y_s becomes comparable to $L/(1 - M^2)^{1/2}$.

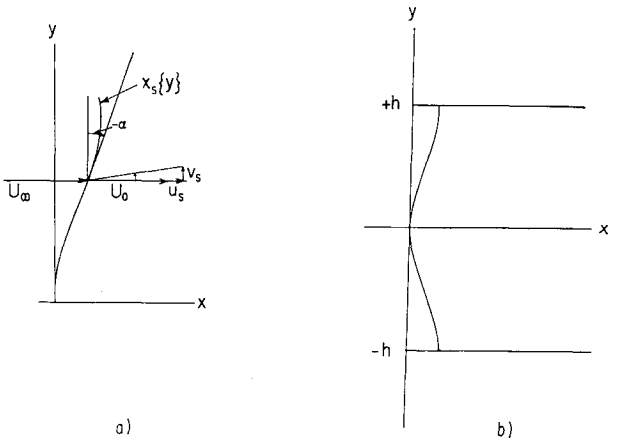

Fig. 2 Geometry and notation for the perturbed normal shock wave.

V. Perturbed Flow Field of an Oblique Shock Wave (Supersonic Wedge Flow)

General Solution

For supersonic wedge flow, $M > 1$, so that Eqs. (11) and (12) are wave equations with source functions determined by the radiative transfer. The general solution is obtained

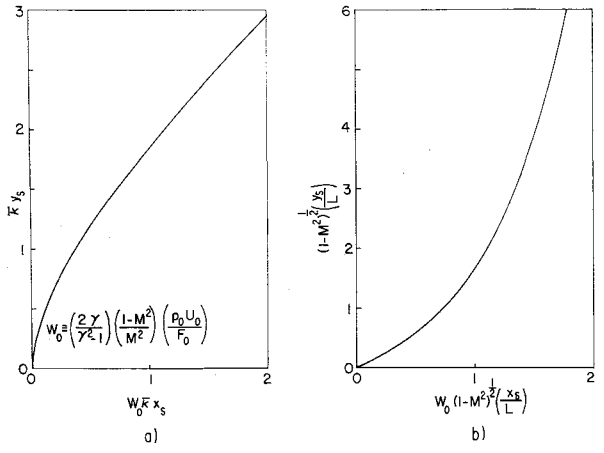

Fig. 3 Shock front curvature of the radiation-perturbed normal shock wave for a) a gray gas in the region $y \ll L/(1\text{-}M^2)^{1/2}$ and b) any gas in the region $y \gg l$.

by integrating the radiation sources over the cross-hatched region shown in Fig. 4. The boundary conditions to be satisfied are $v\{x, 0\} = 0$, and Eqs. (15) at the shock front. The condition $v\{x, 0\} = 0$ is satisfied by placing the source distribution $\epsilon\{x, y\} = \epsilon\{x, |y|\}$ in the negative y region, whereas along the shock-front line and its reflection across the x axis, $y = \pm x \tan\alpha_0$, a line source is placed with a strength $\tilde{\sigma}\{x\}$ which is determined by the requirement that Eqs. (15) be satisfied.

The equations and boundary conditions of this steady, oblique shock-flow problem can be transformed to those of the unsteady normal shock-flow problem considered in Ref. 1. The appropriate transformations are

$$x \tan\alpha_0 \rightarrow U_0 t, \quad (M^2 - 1)^{1/2} \tan\alpha_0 \rightarrow U_0/a, \quad \rho_0 \tan\alpha_0 \rightarrow \rho_0 \tag{35}$$

Use of these transformations on the results of Ref. 1 yields the following solutions:

$$\frac{p}{p_0} = \left(\frac{\rho_0 U_0}{2p_0}\right)\frac{1}{\mu^2}\left[\int_{\xi_2}^{x} \epsilon\left\{\xi, \frac{1}{\mu}(x-\xi)\right\} d\xi + \int_{\xi_1}^{x} \epsilon\left\{\xi, \left|y - \frac{1}{\mu}(x-\xi)\right|\right\} d\xi + \left(\frac{\mu}{1+K}\right)(\sigma'\{\xi_2\} + \sigma'\{\xi_1\})\right] + B\{0\} \tag{36}$$

$$\frac{v}{U_0} = \frac{1}{2U_0\mu}\left[\int_{\xi_2}^{x} \epsilon\left\{\xi, y + \frac{1}{\mu}(x-\xi)\right\} d\xi - \int_{\xi_1}^{x} \epsilon\left\{\xi, \left|y - \frac{1}{\mu}(x-\xi)\right|\right\} d\xi + \left(\frac{\mu}{1+K}\right)(\sigma'\{\xi_2\} - \sigma'\{\xi_1\})\right] \tag{37}$$

where

$$\sigma'\{\xi_{1,2}\} \equiv \tilde{\sigma}\{\xi_{1,2}\} - \tilde{\sigma}\{0\} = \frac{(1+K)}{\mu}\sum_{n=1}^{\infty}\left(\frac{\Gamma'-1}{\Gamma'+1}\right)^n\left[\int_{[(1-K)/(1+K)]^{n-1}\xi_{1,2}}^{[(1-K)/(1+K)]^{n}\xi_{1,2}} \times \epsilon\left\{\xi, \left|\left[\frac{(1-K)^n}{(1+K)^{n-1}}\right]\frac{\xi_{1,2}}{\mu} - \frac{\xi}{\mu}\right|\right\} d\xi - \left(\frac{2p_0}{\rho_0 U_0}\right) \times \left(\frac{\mu^2}{\Gamma'-1}\right)\left[B\left\{x_s = \left(\frac{1-K}{1+K}\right)^{n-1}\xi_{1,2}\right\} - B\{0\}\right]\right] \tag{38}$$

$$K \equiv (M^2-1)^{1/2}\tan\alpha_0 \qquad \mu \equiv (M^2-1)^{1/2}$$

$$\Gamma' \equiv \left(\frac{p_0}{\rho_0 U_0^2}\right)(M^2-1)^{1/2}\Gamma$$

$$\xi_1 \equiv \left(\frac{x - \mu y}{1+K}\right) \qquad \xi_2 \equiv \left(\frac{x + \mu y}{1+K}\right)$$

Integration (at constant y) of Eqs. (2) and (8) with the conditions given by Eqs. (15c) and (15d) yields the following expressions for u and ρ:

$$\frac{u}{U_0} = -\frac{1}{\rho_0 U_0^2}\left\{p\{x, y\} - p\{y\cot\alpha_0, y\} \times \left[1 + \left(\frac{\rho_0 U_0^2}{p_0}\right)\frac{\Omega}{\Gamma}\right]\right\} + D\{x_s = y\cot\alpha_0\} - B\{y\cot\alpha_0\}\frac{\Omega}{\Gamma} \tag{39}$$

$$\frac{\rho}{\rho_0} = \frac{1}{\rho a^2}\left\{p\{x, y\} - p\{y\cot\alpha_0, y\} \times \left[1 - \left(\frac{\rho_0 a^2}{\rho_0}\right)\frac{\Delta}{\Gamma}\right]\right\} + C\{y\cot\alpha_0\} - B\{y\cot\alpha_0\} + \frac{1}{U_0}\int_{y\cot\alpha_0}^{x} \epsilon\{\xi, y\} d\xi \tag{40}$$

The shock angle perturbation and the temperature perturbation can be obtained from Eqs. (15a) and (5), respectively.

Evaluation of the Radiative Transfer Term

The radiation source term $\epsilon\{x, y\}$ is computed from the radiant-energy flux $\mathbf{F}\{x, y\}$ by the relation

$$\epsilon\{x, y\} = [z/(fk + z)](1/p_0)\nabla\cdot\mathbf{F}\{x, y\} \tag{41}$$

In order to determine the flux at a point (x, y) in the wedge-shaped shock layer, radiation from all the regions 1–5 shown in Fig. 5 must be considered. The radiation flux at (x, y) is computed by first integrating the radiation emitted along a radius vector, attenuated by absorption between the emitting point and the point (x, y), and then integrating over all directions for the radius vector. For computing the emission and absorption, this study considers a gray gas and a gas with a spectrum consisting of nonoverlapping collision-broadened lines. Also, the wedge surface may emit radiation or diffusely reflect radiation from the shock layer.

For the case of a gray gas, straightforward but somewhat tedious calculation gives the following result:

$$\epsilon = 2\left(\frac{z}{fk+z}\right)\left(\frac{\bar{k}\sigma T_0^4}{p_0}\right)\left[cE_2\{\bar{k}y\} + E_2\{\bar{k}(x\tan\alpha_0 - y)\cos\alpha_0\} - \frac{1}{\pi}(x^2+y^2)^{-1/2}\int_0^1 e^{-\bar{k}(x^2+y^2)^{1/2}/\mu} \times \left\{cy\cos^{-1}\left[\frac{\mu x}{(x^2+y^2-\mu^2y^2)^{1/2}}\right] + (x\sin\alpha_0 - y\cos\alpha_0) \times \cos^{-1}\left[\frac{\mu(x\cos\alpha_0 + y\sin\alpha_0)}{[(x^2+y^2) - \mu^2(x\sin\alpha_0 - y\cos\alpha_0)^2]^{1/2}}\right]\right\} d\mu\right] \tag{42}$$

where $\bar{k}$ is the constant absorption coefficient and σ is the Stefan-Boltzmann constant. The factor c, which determines the effect of surface emission and diffuse reflection, is given by

$$c = 1 - e_s\left(\frac{T_s}{T_0}\right)^4 - r_s\left\{[1 - 2E_3\{\bar{k}x\sin\alpha_0\}]\cos\alpha_0 + \sin^2\alpha_0\left[1 - \frac{2}{\pi}\int_0^1 e^{-\bar{k}x/\mu}(1-\mu^2)^{1/2}d\mu - \frac{2}{\pi}\cos\alpha_0\int_0^1 (1 - e^{-\bar{k}x/\mu})\cos^{-1}\left[\frac{\mu\sin\alpha_0\cos\alpha_0}{(1-\mu^2\sin^2\alpha_0)^{1/2}}\right]\mu d\mu\right]\right\} \tag{43}$$

where e_s, T_s, and r_s are the surface emissivity, temperaturs, and reflectivity, respectively. The functions E_2 and E_3 are the $n = 2$ and $n = 3$ cases of the general exponential integral E_n defined by

$$E_n\{t\} \equiv \int_0^1 w^{n-2}e^{-t/w}dw \tag{44}$$

A short table of E_n values is given in Ref. 9. If the constant

absorption coefficient $\bar{k}$ extends over the spectral region between the frequencies ν_1 and ν_2 rather than over the entire spectrum, then the total blackbody radiancy σT_0^4 appearing in Eq. (42) should be replaced by the integral of the spectral blackbody radiancy R_ν° between ν_1 and ν_2. As mentioned in Sec. IV, several such bands with different $\bar{k}$ values can be accounted for by adding the perturbations, which are computed separately for each band.

For this gray-gas case, it is of interest to consider the forms of ϵ and c in the transparent gas and "optically thick" gas limits. In the transparent gas limit ($\bar{k}x \ll 1$), Eqs. (42) and (43) reduce to

$$\epsilon = 4\left(\frac{z}{fk+z}\right)\left(\frac{\bar{k}\sigma T_0^4}{p_0}\right)\left[1 - \left(\frac{\alpha_0}{2\pi}\right) - \left(\frac{1-c}{2}\right)\times \left(1 - \frac{1}{\pi}\tan^{-1}\left\{\frac{y}{x}\right\}\right)\right] \quad (45)$$

and

$$c = 1 - e_s\left(\frac{T_s}{T_0}\right)^4 - r_s\frac{\sin^2\alpha_0}{2} \quad (46)$$

In Eq. (45), the factor $\alpha_0/2\pi$ arises from the fact that there will be an infinite wedge-shaped region of angle α_0 (region 3 in Fig. 5) contributing radiation to any point (x, y). For a wedge of finite length, the factor $\alpha_0/2\pi$ would disappear for $\bar{k}$ small enough. Even for the infinite wedge, however, $\alpha_0/2\pi$ will be small enough to neglect for all practical cases; e.g., for $\alpha_0 = 10°$, 20°, and 30°, $\alpha_0/2\pi$ becomes less than 0.03, 0.06, and 0.09, respectively. It should be noted that α_0 will be quite small for all cases of interest; the maximum values of α_0 for an attached shock wave in the strong shock limit, $M\sin\alpha_0 = [(\gamma-1)/2\gamma]^{1/2}$ are 26.6°, 22.2°, and 16.8° for γ values of 1.67, 1.4, and 1.2, respectively (the effective value of γ for a strong shock in air is often 1.2 or lower because of real gas effects). A typical example is the calculation of Ref. 2 for a wedge of 35° half angle traveling at $M_\infty = 60$ and 60 km, which yields $\alpha_0 \simeq 7°$. In Eq. (45) we shall also neglect the $(1/\pi)\tan^{-1}(y/x)$ term, which is less than or equal to α_0/π. The $r_s\sin^2\alpha_0/2$ term in Eq. (46), which arises from the reflection of radiation from the infinite region of angle α_0 adjacent to the surface, can similarly be neglected, since $r_s \leq 1$. Accordingly, the following expression will be used in the transparent gas limit:

$$\epsilon = 4\left(\frac{z}{fk+z}\right)\left(\frac{\bar{k}\sigma T_0^4}{p_0}\right)\left[1 - \frac{e_s}{2}\left(\frac{T_s}{T_0}\right)^4\right] \quad (47)$$

The surface radiation will reduce the flow field perturbations by the factor $(e_s/2)(T_s/T_0)^4$, whereas the surface reflectivity has no effect in the transparent gas limit.

In the limit of an "optically thick" gas ($\bar{k}x\tan\alpha_0 \gg 1$), the radiative transfer source term ϵ reduces to just the first two terms on the right-hand side of Eq. (42). The surface emission and reflection factor c reduces to

$$c = 1 - e_s(T_s/T_0)^4 - r_s \quad (48)$$

The surface emission and reflection will therefore modify, by the preceding amount, only the flow field perturbations determined by the $E_2\{\bar{k}y\}$ term of Eq. (42). The $E_2\{\bar{k}y\}$ term will produce perturbations which vary only within a few photon mean free paths of the wedge surface and constant perturbations across the shock layer.

In the transparent gas limit, the two E_2 terms contributed the terms that were retained in Eq. (47), whereas the remaining integral in Eq. (42) contributed the terms that were shown to be negligible, and therefore omitted from Eq. (47). As the gas becomes absorbing, it can be shown that the integral in Eq. (42) decreases faster than the E_2 terms. Therefore, at all values of optical depth, ϵ can be very well approximated by just the E_2 terms. Since $\cos\alpha_0$ is very near unity for the values of α_0 of interest (e.g., $\cos 20° =$ 0.94), it will be replaced by unity in our calculations in order to obtain the following expression:

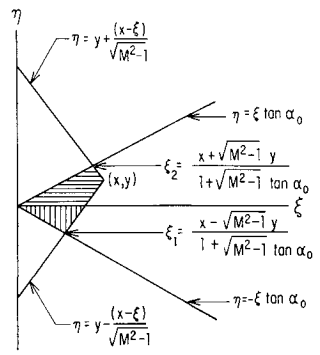

Fig. 4 Diagram of the $\xi\eta$ plane showing the region of radiation sources for the calculation of the perturbations behind the oblique shock wave.

$$\epsilon = 2\left(\frac{z}{fk+z}\right)\left(\frac{\bar{k}\sigma T_0^4}{p_0}\right)\times [cE_2\{\bar{k}y\} + E_2\{\bar{k}(x\tan\alpha_0 - y)\}] \quad (49)$$

This is the expression we would calculate for ϵ by assuming the shock layer to be a slab with constant thickness equal to the shock-layer height $y_s = x\tan\alpha_0$ at x (see Fig. 5). Similarly, the factor c can be accurately approximated at all optical depths by the constant thickness slab value

$$c = 1 - e_s(T_s/T_0)^4 - r_s[1 - 2E_3\{\bar{k}x\tan\alpha_0\}] \quad (50)$$

Since the effect of surface emission and reflection in the transparent and optically thick limits has been determined previously, all of the following calculations will neglect surface emission and reflection [thus Eq. (50) will not be utilized].

The radiation from spectral lines can make an important contribution to the total radiant-energy flux. When the lines are transparent or well overlapped, the transparent and gray-gas approximations, respectively, may be used. The absorption coefficient at a line center is generally quite large, so absorption is often important for line radiation. Accordingly, radiation in the form of self-absorbed nonoverlapping spectral lines will now be considered. If appreciable self-absorption occurs, then the line profile in the wings (i.e., away from the line center) will determine the radiative transfer. The absorption coefficient in the wings of a spectral line will be determined by collision broadening unless the temperature is high enough to cause sufficient ionization for Stark broadening to be dominant (it will be shown below that Stark broadening will give nearly the same results as collision broadening). Doppler broadening is important near the line center, and will not affect the absorption very far out into the wings unless the pressure is very low and the line is not very strongly self-absorbed.

The spectral absorption coefficient for a collision-broadened line is (see, e.g., Ref. 10)

$$k_\nu = \frac{S}{\pi}\frac{b}{(\nu-\nu_0)^2 + b^2} \quad (51)$$

where $S = \int k_\nu d\nu$ is the integrated intensity of the line, ν_0 is the frequency at the line center, and b is the line half-width (here defined as $|\nu_{1/2} - \nu_0|$, where $\nu_{1/2}$ is the frequency at which $k_\nu = \frac{1}{2}k_{\nu_0}$). For radiation path lengths greater than about $4b/S$, the center of the line will be strongly self-

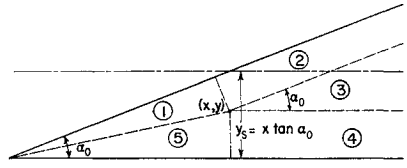

Fig. 5 Geometry and notation used in calculating the radiative transfer for the oblique shock wave.

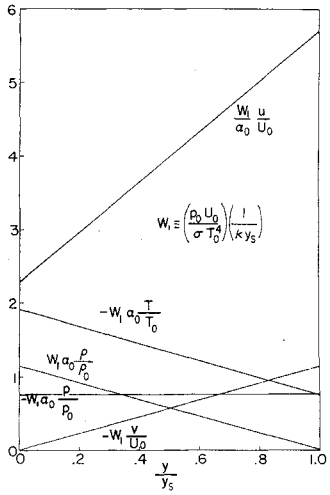

Fig. 6 The perturbations across an oblique shock layer in the limit of a strong shock and $\alpha_0 \to 0$ for a transparent, perfect gas with $\gamma = 1.67$.

absorbed, with the result that the b^2 term in the denominator of Eq. (51) can be neglected compared with $(\nu - \nu_0)^2$ [this results in an absorption along path r which is proportional to $r^{1/2}$ and which is very near the value of the absorption computed using the entire Eq. (51)]. Except within a distance of about $4b/S$ of the shock front and wedge surface, the radiative transfer term becomes

$$\epsilon = \frac{4}{3}\left(\frac{z}{fk+z}\right)\left(\frac{\sigma T_0^4}{p_0}\right)\frac{(Sb)^{1/2}}{d^*}\left[y^{-1/2} + [(x\tan\alpha_0 - y)\times \cos\alpha_0]^{-1/2} - \frac{3}{2\pi}(x^2+y^2)^{-3/4}\int_0^1 \left\{ y \times \cos^{-1}\left[\frac{\mu x}{x^2+y^2-\mu^2 y^2}\right] + (x\sin\alpha_0 - y\cos\alpha_0)\times \cos^{-1}\left[\frac{\mu(x\cos\alpha_0 + y\sin\alpha_0)}{(x^2+y^2-\mu^2(x\sin\alpha_0 - y\cos\alpha_0)^2)^{1/2}}\right]\right\}\mu^{1/2}d\mu\right] \quad (52)$$

Surface emission and reflection has been neglected, and the spectrum is assumed to consist of equally intense spectral lines equally spaced at a distance d^* apart throughout the entire spectrum. If the lines don't cover the entire spectrum, then $\sigma T_0^4/d^*$ should be replaced by $N\langle R_\nu^0\rangle$, where N is the total number of lines and $\langle R_\nu^0\rangle$ is the average spectral radiancy at the line centers. If the lines have unequal intensities and half-widths, then $N\langle R_\nu^0(Sb)^{1/2}\rangle$ should be used. Thus, by combining these perturbations with those for transparent and gray gases, a quite general system of continuum and line radiation (nonoverlapped and well-overlapped lines) can be considered. By replacing the $\cos^{-1}$ terms in Eq. (52) by their maximum values of $\pi/2$, the ratio of the first term under the integral to the $y^{-1/2}$ term is shown to be less than $\frac{1}{2}[y/(x^2+y^2)^{1/2}]^{3/2}$, whereas the ratio

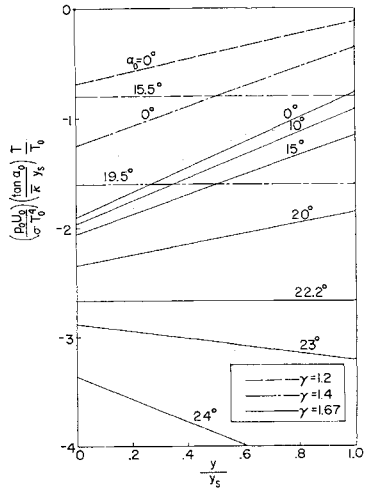

Fig. 7 The temperature perturbation across an oblique shock layer for various shock-layer angles α_0 in the limit of a strong shock in a transparent, perfect gas.

of the second term under the integral to $[(x\tan\alpha_0 - y)\cos\alpha_0]^{-1/2}$ is less than $\frac{1}{2}[(x\tan\alpha_0 - y)\cos\alpha_0/(x^2+y^2)^{1/2}]^{3/2}$. The upper limit for the first ratio goes from zero at the wedge surface to a maximum value of $\frac{1}{2}(\sin\alpha_0)^{3/2}$ at the shock front, whereas that for the second ratio goes from zero at the shock front to $\frac{1}{2}(\sin\alpha_0)^{3/2}$ at the wedge surface. Since $\frac{1}{2}(\sin 20°)^{3/2} = 0.10$, it is seen that the integral in Eq. (52) can be neglected. Since $\cos\alpha_0$ will be near unity for all cases of interest, Eq. (52) reduces to the following expression, which is equivalent to the radiative transfer term for a slab of constant thickness $y_s = x\tan\alpha_0$:

$$\epsilon = \frac{4}{3}\left(\frac{z}{fk+z}\right)\left(\frac{\sigma T_0^4}{p_0}\right)\frac{(Sb)^{1/2}}{d^*}\left[y^{-1/2} + (x\tan\alpha_0 - y)^{-1/2}\right] \quad (53)$$

The simple theory for Stark broadening gives a line profile that decreases as $(\nu - \nu_0)^{-5/2}$ in the wings, rather than as the collision broadening form $(\nu - \nu_0)^{-2}$. This $\frac{5}{2}$-power dependence will therefore produce an expression for ϵ similar to Eq. (53) but with $y^{-1/2}$ and $(x\tan\alpha_0 - y)^{-1/2}$ replaced by $y^{-0.6}$ and $(x\tan\alpha_0 - y)^{-0.6}$, respectively. Since the form of ϵ for Stark broading will not differ appreciably from that for collision broadening, we shall carry through calculations only for collision-broadening.

Solutions for Various Types of Radiating Gases

As discussed in the preceding section, the radiation source term ϵ for the wedge-shaped shock layer can be accurately approximated by ϵ for an infinite layer of constant thickness, as given by Eqs. (47, 49, and 53) for a transparent gas, a gray gas, and a gas with nonoverlapping collision-broadened lines, respectively. The infinite slab of constant thickness is the same geometry appearing in the unsteady, normal shock problem considered in Ref. 1. Accordingly, the results for transparent and gray gases can be obtained directly from Ref. 1 by means of the transformations (35). The case of nonoverlapping lines was not considered in Ref. 1, so the results obtained in this paper can be transformed to obtain the flow field perturbations for the unsteady normal shock wave. In all of the following calculations, it is assumed that radiation ahead of the shock is unimportant ($A = B = C = D = 0$), and the effects of surface emission and reflection are not included (see the preceding section for a discussion of the effects of surface emission and reflection).

Transparent gas

The following flow field perturbations for a transparent gas can be obtained from Ref. 1 by the transformations (35), or by integration of Eqs. (36) and (37) for the constant radiation source term given in Eq. (47):

$$\frac{p}{p_0} = -4\left(\frac{z}{fk+z}\right)\left(\frac{\rho_0 U_0^2}{p_0}\right)\left(\frac{\sigma T_0^4}{\rho_0 U_0}\right)\times \left(\frac{1}{M^2-1}\right)\left(\frac{\Gamma' K}{1+\Gamma' K}\right)\bar{k}x \quad (54)$$

$$\frac{v}{U_0} = -4\left(\frac{z}{fk+z}\right)\left(\frac{\sigma T_0^4}{\rho_0 U_0}\right)\left(\frac{1}{1+\Gamma' K}\right)\bar{k}y \quad (55)$$

where we recall that $K = (M^2-1)^{1/2}\tan\alpha_0$. The perturbations u, ρ, and T are easily computed from Eqs. (39, 40, and 5), respectively, and are seen to be linear functions of both variables x and y. For a perfect gas,

$$\left(\frac{z}{fk+z}\right) = \left(\frac{\gamma-1}{\gamma}\right) \qquad \left(\frac{\rho_0 U_0^2}{p_0}\right) = \gamma M^2$$

and our results agree with those of Ref. 2 upon changing to their notation, $p \to \rho_0 U_0 p'$, $v \to U_0 v'$, $\Gamma \to \gamma(M^2-1)^{1/2}$, $x \to x'L$, $y \to y'L$, and $\epsilon = 4[z/(fk+z)](\bar{k}\sigma T_0^4/p_0) \to WU_0/L$. Reference 2 solves the problem only for the case

of a transparent gas. It should be noted that all perturbations calculated in this paper will be proportional to the parameter $(\sigma T_0^4/p_0U_0)$, which is a measure of the radiant-energy loss compared with the energy of the shocked gas.

In the limit of a strong shock ($M \sin\alpha_0 = [(\gamma - 1)/2\gamma]^{1/2}$) and a very slender shock layer ($\alpha_0 \ll 1$), the perturbations take on the following values for a perfect gas:

$$\left.\begin{aligned} W_1\alpha_0 \frac{p}{p_0} &= -4\frac{(\gamma-1)^2}{2\gamma-1} \\ W_1\alpha_0 \frac{\rho}{\rho_0} &= 4\left(\frac{\gamma-1}{2\gamma-1}\right)(1-r) \\ W_1\alpha_0 \frac{T}{T_0} &= -4\left(\frac{\gamma-1}{2\gamma-1}\right)(\gamma-r) \\ W_1 \frac{v}{U_0} &= -4\left(\frac{\gamma-1}{2\gamma-1}\right) r \\ \frac{W_1}{\alpha_0}\frac{u}{U_0} &= \left(\frac{8}{2\gamma-1}\right)[(\gamma-1)+r] \end{aligned}\right\} \quad (56)$$

where $W_1 \equiv (p_0U_0/\sigma T_0^4)(1/\bar{k}y_s)$, $r \equiv y/y_s$, and $y_s = x\tan\alpha_0$ is the layer thickness at x. Equations (56) are plotted in Fig. 6 for $\gamma = 1.67$. Since $\alpha_0 \ll 1$, the velocity perturbations u/U_0 and v/U_0 will be much smaller than p/p_0, ρ/ρ_0, and T/T_0.† The perturbation p is constant across the shock layer, being a function of x only; thus, only T and ρ vary appreciably across the shock layer. This qualitative result was obtained in Refs. 11 and 12 for similarity solutions of hypersonic flow past slender bodies. The blunt-body studies of Refs. 3–7 also report that the primary effect of the radiation is to change the density and temperature distributions, with the velocities remaining relatively unchanged.

The perturbation temperature for a perfect gas is given by

$$\left(\frac{p_0U_0}{\sigma T_0^4}\right)\left(\frac{\tan\alpha_0}{\bar{k}y_s}\right)\frac{T}{T_0} = -4\left(\frac{\gamma-1}{\gamma}\right)\left\{\left[1+(\gamma-1)\left(\frac{M^2}{M^2-1}\right)\left(\frac{\Gamma' K}{1+\Gamma' K}\right)\right] - \left[1-\left(\frac{M^2}{M^2-1}\right)\left(\frac{\Gamma' K}{1+\Gamma' K}\right)\right] r\right\} \quad (57)$$

In the strong shock limit shown in Fig. 7, the temperature decreases linearly with distance behind the shock front for small values of α_0, but as α_0 increases, the temperature decreases more rapidly at the shock front than at the wedge surface, so that eventually a constant temperature distribution across the shock layer is reached. This occurs for the angle α_0^* given by $\sin^2\alpha_0^* = \frac{1}{2}[(\gamma - 1)/(2\gamma - 1)]$. At large values of α_0, the temperature is lower at the shock front than at the surface, with the temperature perturbation diverging to $-\infty$ when $M = 1$, i.e., at the maximum angle for an attached shock: $\sin^2\alpha_{0,\max} = [(\gamma - 1)/2\gamma]$. Since the pressure is constant across the shock layer, the preceding conclusions show that the density will be greatest at the surface only for $\alpha_0 < \alpha_0^*$.

Figure 8 illustrates the effect of shock strength on the temperature distribution. The top part of the figure shows that, as γ approaches unity, the strong and weak shock perturbations for a given α_0 become identical and approach zero. Analytically this result is

$$\left(\frac{p_0U_0}{\sigma T_0^4}\right)\left(\frac{\tan\alpha_0}{\bar{k}y_s}\right)\left(\frac{T}{T_0}\right)_{\gamma\to 1} = 4\left(\frac{\gamma-1}{\gamma}\right)(1-r) \quad (58)$$

† Here we are considering values of γ which are not near unity, and so the requirement $\alpha_0 \ll 1$ implies slender wedges. If $(\gamma - 1) \ll 1$, then Eqs. (56) will be applicable for nonslender wedges, since α_0 will be of order $(\gamma - 1)$. For this $(\gamma - 1) \ll 1$ case, the perturbations p/p_0, u/U_0, and v/U_0 will be smaller than ρ/ρ_0 and T/T_0, by factors of order $(\gamma - 1)$.

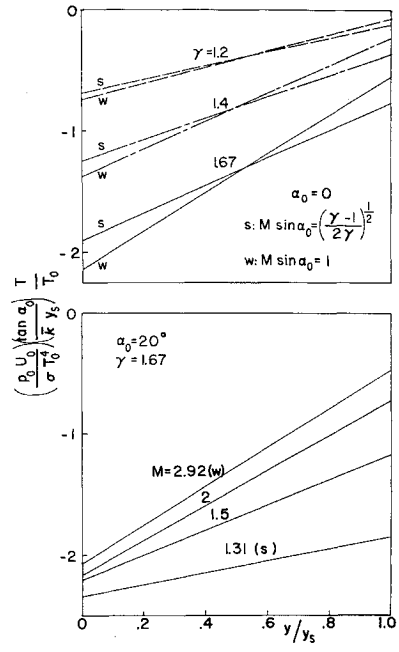

Fig. 8 The temperature perturbation across an oblique shock layer for various shock strengths in a transparent, perfect gas.

with all the terms dependent on the shock strength and α_0 going to zero as $(\gamma - 1)^2$ or faster. Comparison of the curves in Fig. 8 for $\alpha_0 = 0°$ with those for 20° illustrates the fact that the weak shock temperature distribution is nearly independent of α_0.

Gray gas

Use of the transformations (35) on the results of Ref. 1, or integration of Eqs. (36) and (37) for the radiation source term given in Eq. (49), yields the following perturbations for a gray gas:

$$\begin{aligned} \frac{p}{p_0} = &-\left(\frac{z}{fk+z}\right)\left(\frac{\rho_0U_0^2}{p_0}\right)\left(\frac{\sigma T_0^4}{p_0U_0}\right)\frac{1}{\mu}\left[\left(\frac{2+K}{1+K}\right) - E_3\left\{\left(\frac{K}{1+K}\right)\bar{k}\left(\frac{x}{\mu}+y\right)\right\} - E_3\left\{\left(\frac{K}{1+K}\right)\bar{k}\times\left(\frac{x}{\mu}-y\right)\right\} + \left(\frac{2K}{1-K^2}\right)E_3\left\{\bar{k}\left(K\frac{x}{\mu}-y\right)\right\} - \left(\frac{2}{1-K^2}\right)E_3\left\{K\bar{k}\left(\frac{x}{\mu}-y\right)\right\} + \sum_{n=1}^{\infty}\left(\frac{\Gamma'-1}{\Gamma'+1}\right)^n\times\left[2\left(\frac{2-K^2}{1-K^2}\right) - E_3\left\{\left(K\frac{(1-K)^n}{(1+K)^{n+1}}\right)\bar{k}\left(\frac{x}{\mu}+y\right)\right\} - E_3\left\{\left(K\frac{(1-K)^n}{(1-K)^{n+1}}\right)\bar{k}\left(\frac{x}{\mu}-y\right)\right\} - E_3\left\{\left(K\frac{(1-K)^{n-1}}{(1+K)^n}\right)\bar{k}\left(\frac{x}{\mu}+y\right)\right\} - E_3\left\{\left(K\frac{(1-K)^{n-1}}{(1+K)^n}\right)\bar{k}\left(\frac{x}{\mu}-y\right)\right\} - \left(\frac{2}{1-K^2}\right)\left(E_3\left\{K\left(\frac{1-K}{1+K}\right)^n\bar{k}\left(\frac{x}{\mu}+y\right)\right\} + E_3\left\{K\left(\frac{1-K}{1+K}\right)^n\bar{k}\left(\frac{x}{\mu}-y\right)\right\}\right)\right]\right] \end{aligned} \quad (59)$$

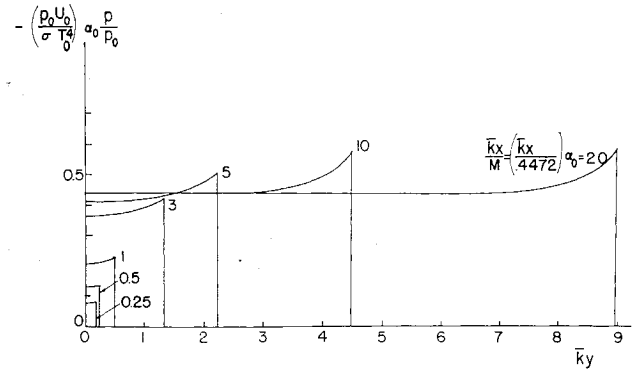

Fig. 9 The pressure perturbation across an oblique shock layer at various distances from the wedge vertex in the limit of a strong shock for a gray, perfect gas with $\gamma = 1.67$.

$$\frac{v}{U_0} = -\left(\frac{z}{fk+z}\right)\left(\frac{\sigma T_0^4}{p_0U_0}\right)\left\{1 - 2E_3\{\bar{k}y\} + E_3\left\{\left(\frac{K}{1+K}\right)\bar{k}\left(\frac{x}{\mu}+y\right)\right\} - E_3\left\{\left(\frac{K}{1+K}\right)\bar{k}\times\left(\frac{x}{\mu}-y\right)\right\} + \left(\frac{2}{1-K^2}\right)\left[E_3\left\{\bar{k}\left(K\frac{x}{\mu}-y\right)\right\} - E_3\left\{K\bar{k}\left(\frac{x}{\mu}-y\right)\right\}\right] + \sum_{n=1}^{\infty}\left(\frac{\Gamma'+1}{\Gamma'+1}\right)^n\times\left[E_3\left\{\left(K\frac{(1-K)^n}{(1+K)^{n+1}}\right)\bar{k}\left(\frac{x}{\mu}+y\right)\right\} - E_3\left\{\left(K\frac{(1-K)^n}{(1+K)^{n+1}}\right)\bar{k}\left(\frac{x}{\mu}-y\right)\right\} + E_3\left\{\left(K\frac{(1-K)^{n-1}}{(1+K)^n}\right)\bar{k}\left(\frac{x}{\mu}+y\right)\right\} - E_3\left\{\left(K\frac{(1-K)^{n-1}}{(1+K)^n}\right)\bar{k}\left(\frac{x}{\mu}-y\right)\right\} + \left(\frac{2}{1-K^2}\right)\left(E_3\left\{K\left(\frac{1-K}{1+K}\right)^n\bar{k}\left(\frac{x}{\mu}+y\right)\right\} - E_3\left\{K\left(\frac{1-K}{1+K}\right)^n\bar{k}\left(\frac{x}{\mu}-y\right)\right\}\right)\right]\right\} \quad (60)$$

These expressions for the pressure and y-velocity perturbations are plotted in Figs. 9 and 10, respectively, for a perfect gas in the limit of a strong shock and $\alpha_0 \to 0$. Figure 9 shows that the pressure perturbation builds up linearly with increasing x and is independent of y for small x (transparent gas regime), whereas at very large distances from the wedge vertex (optically thick gas regime), the pressure perturbation is constant except for a region of length equal to about two photon mean free paths at the shock front. The $E_3\{\bar{k}[K(x/\mu) - y]\} \equiv E_3\{\bar{k}(y_s - y)\}$ term in Eq. (59) produces this profile near the shock front. The gas y-velocity perturbation v is shown in Fig. 10 to increase linearly with y, independent of x, in the transparent regime (dotted line), whereas for large x, v is constant except for two boundary regions, one at the wedge surface and the other at the shock front. It is seen from Eq. (60) that the wedge boundary profile is given by the $E_3\{\bar{k}y\}$ term, whereas the shock boundary profile is given by the $E_3\{\bar{k}[K(x/\mu) - y]\} \equiv E_3\{\bar{k}(y_s - y)\}$ term. Since the shock angle perturbation α is proportional to the value of the y-velocity perturbation v at the shock front [cf., Eq. (15a)], reference to Fig. 10 shows that $-\alpha$ will increase linearly with y_s at small $\bar{k}y_s$ and will level off to a constant value when $\bar{k}y_s$ becomes greater than about five, i.e., when the shock-layer thickness becomes equal to about five photon mean free paths.

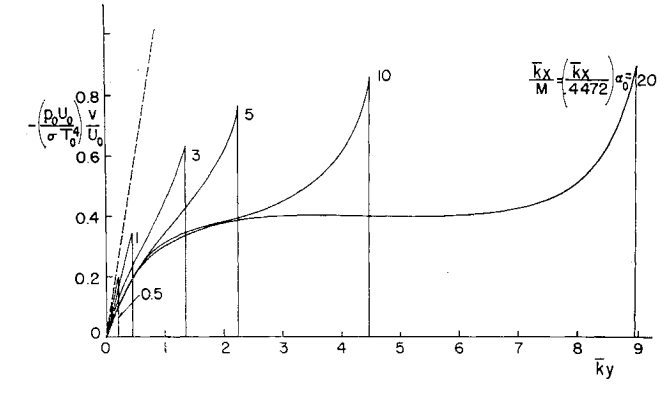

Fig. 10 The y-velocity perturbation across an oblique shock layer at various distances from the wedge vertex in the limit of a strong shock for a gray, perfect gas with $\gamma = 1.67$.

In the "optically thick" limit all of the flow field perturbations will approach constant values, except for profiles at the wedge surface and at the shock front, with each profile having a length equal to about two photon mean free paths. For a perfect gas in the limit of a strong shock and $\alpha_0 \to 0$, the perturbations for the optically thick shock layer become

$$\begin{aligned}
\left(\frac{p_0U_0}{\sigma T_0^4}\right)\alpha_0\frac{p}{p_0} &= -\frac{(\gamma-1)^2}{\gamma(\gamma+1)}\left[(2\gamma+1) + 2\gamma E_3\{\bar{k}(y_s-y)\}\right] \\
\left(\frac{p_0U_0}{\sigma T_0^4}\right)\alpha_0\frac{\rho}{\rho_0} &= \left(\frac{\gamma-1}{\gamma}\right)\left[2\bar{k}(y_s-y)E_2\{\bar{k}y\} + \left(\frac{2\gamma}{\gamma+1}\right)(1 - E_3\{\bar{k}(y_s-y)\})\right] \\
\left(\frac{p_0U_0}{\sigma T_0^4}\right)\alpha_0\frac{T}{T_0} &= -\left(\frac{\gamma-1}{\gamma}\right)\left[(2\gamma-1) + 2\bar{k}(y_s-y)E_2\{\bar{k}y\} - 2\gamma\left(\frac{3-\gamma}{\gamma+1}\right)E_3\{\bar{k}(y_s-y)\}\right] \\
\left(\frac{p_0U_0}{\sigma T_0^4}\right)\frac{v}{U_0} &= -\left(\frac{\gamma-1}{\gamma}\right)\left[1 - 2E_3\{\bar{k}y\} + \left(\frac{4\gamma}{\gamma+1}\right)E_3\{\bar{k}(y_s-y)\}\right] \\
\left(\frac{p_0U_0}{\sigma T_0^4}\right)\frac{1}{\alpha_0}\frac{u}{U_0} &= 4\left[1 + \left(\frac{\gamma-1}{\gamma+1}\right)E_3\{\bar{k}(y_s-y)\}\right]
\end{aligned} \quad (61)$$

Equations (61) are plotted for $\gamma = 1.67$ in Fig. 11, which shows the profiles at the shock front and at the wedge surface, as well as the constant values in between. Again we see that the velocity perturbations will be appreciably smaller than the temperature, density, and pressure perturbations since $\alpha_0 \ll 1$. Figure 11 shows that near the shock front the T, ρ, and p perturbations will all be the same order of magnitude, with T and ρ showing somewhat more variation than p. Near the wedge surface, the perturbations T and ρ will grow linearly with $\bar{k}y_s$, and thus in this optically thick limit ($ky_s \gg 1$) these perturbations will be appreciably greater than any other perturbations in the flow field. These large T and ρ perturbations near the wedge surface arise from the fact that the gas flowing near the surface will be continuously losing energy by radiation at constant pressure, whereas near the shock front, a gas element will lose energy only while it flows through the region extending to a couple of photon mean free paths behind the shock front.

The perturbations T and ρ near the wedge surface will be independent of the shock-wave properties, depending only on

the distance x from the wedge vertex where the gas passed through the shock front. Thus, for all M and α_0

$$\left(\frac{p_0U_0}{\sigma T_0^4}\right)\frac{T}{T_0} = -\left(\frac{p_0U_0}{\sigma T_0^4}\right)\frac{\rho}{\rho_0} = -2\left(\frac{\gamma-1}{\gamma}\right)\bar{k}x\,E_2\{\bar{k}y\} \tag{62}$$

The temperature perturbation near the shock front will depend on the shock-wave properties according to the relation

$$\left(\frac{p_0U_0}{\sigma T_0^4}\right)\tan\alpha_0\frac{T}{T_0} = -\left(\frac{\gamma-1}{\gamma}\right)\left[\left\{1+\left(\frac{M^2}{M^2-1}\right)\times\left[\left(1-\gamma\frac{\Delta}{\Gamma}\right)\left(\frac{K^2}{1-K^2}\right)+\gamma\left(1-\frac{\Delta}{\Gamma}\right)\times\left(\frac{(2-K^2)\Gamma'K-K^2}{1-K^2}\right)\right]\right\}-2\left\{1-(\gamma-1)\left(\frac{M^2}{M^2-1}\right)\times\left(\frac{K^2}{1-K^2}\right)\right\}E_3\{\bar{k}(y_s-y)\}\right] \tag{63}$$

The top part of Fig. 12 for the limit of a strong shock shows that changing α_0 will change the temperature perturbation by a constant amount, without affecting the profile. Varying the shock strength, as shown in the lower part of Fig. 12, will change the profile in a manner similar to the way in which a variation in α_0 will change the temperature profile for a transparent gas (cf., Fig. 7).

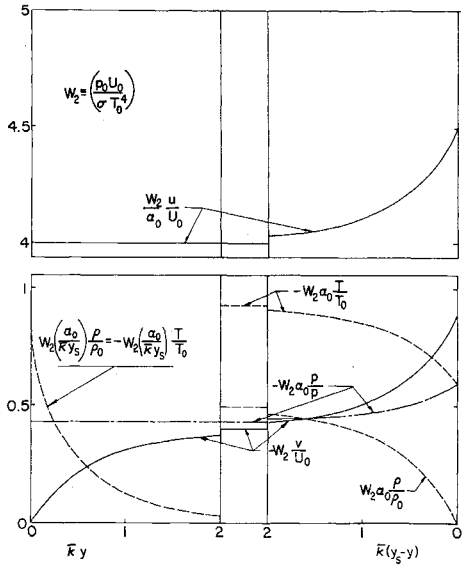

Fig. 11 The perturbations across an oblique shock layer in the limit of a strong shock and $\alpha_0 \to 0$ for an optically thick, gray, perfect gas with $\gamma = 1.67$.

Collision-broadened nonoverlapping lines

For the nonoverlapping line case, substitution of Eq. (53) into Eqs. (36) and (37) yields the following perturbations:

$$\frac{p}{p_0} = -\frac{4}{3}\left(\frac{z}{fk+z}\right)\left(\frac{\rho_0U_0^2}{p_0}\right)\left(\frac{\sigma T_0^4}{p_0U_0}\right)\frac{(Sb)^{1/2}}{d^*}\frac{1}{\mu}\left\{\left(\frac{K}{1+K}\right)^{1/2}\left(\frac{x}{\mu}+y\right)^{1/2}+K^{1/2}\left[\left(\frac{1}{1+K}\right)^{1/2}+\left(\frac{2}{1-K^2}\right)\right]\left(\frac{x}{\mu}-y\right)^{1/2}-\left(\frac{2K}{1-K^2}\right)\left(K\frac{x}{\mu}-y\right)^{1/2}-\left[\frac{1+[(1+K)/(1-K)]^{1/2}+[1/(1+K)^{1/2}]+[(1+K)^{1/2}/(1-K)]}{1+[(1+\Gamma')/(1-\Gamma')][(1+K)/(1-K)]^{1/2}}\right]\times\left(\frac{K}{1+K}\right)^{1/2}\left[\left(\frac{x}{\mu}+y\right)^{1/2}+\left(\frac{x}{\mu}-y\right)^{1/2}\right]\right\} \tag{64}$$

$$\frac{v}{U_0} = -\frac{4}{3}\left(\frac{z}{fk+z}\right)\left(\frac{\sigma T_0^4}{p_0U_0}\right)\frac{(Sb)^{1/2}}{d^*}\left\{2y^{1/2}-\left(\frac{K}{1+K}\right)^{1/2}\left(\frac{x}{\mu}+y\right)^{1/2}+K^{1/2}\left[\left(\frac{1}{1+K}\right)^{1/2}\left(\frac{2}{1-K^2}\right)\right]\left(\frac{x}{\mu}-y\right)^{1/2}-\left(\frac{2}{1-K^2}\right)\left(K\frac{x}{\mu}-y\right)^{1/2}+\left[\frac{1+[(1+K)/(1-K)]^{1/2}+[1/(1+K)^{1/2}]+[(1+K)^{1/2}/(1-K)]}{1+[(1+\Gamma')/(1+\Gamma')][(1+K)/(1-K)]^{1/2}}\right]\times\left(\frac{K}{1+K}\right)^{1/2}\left[\left(\frac{x}{\mu}+y\right)^{1/2}-\left(\frac{x}{\mu}-y\right)^{1/2}\right]\right\} \tag{65}$$

Since Eq. (53) assumes that the lines have radiation path lengths greater than about $4b/S$ to insure sufficient absorption, our expressions for the perturbations will be accurate except within a distance of about $4b/S$ of the shock front or

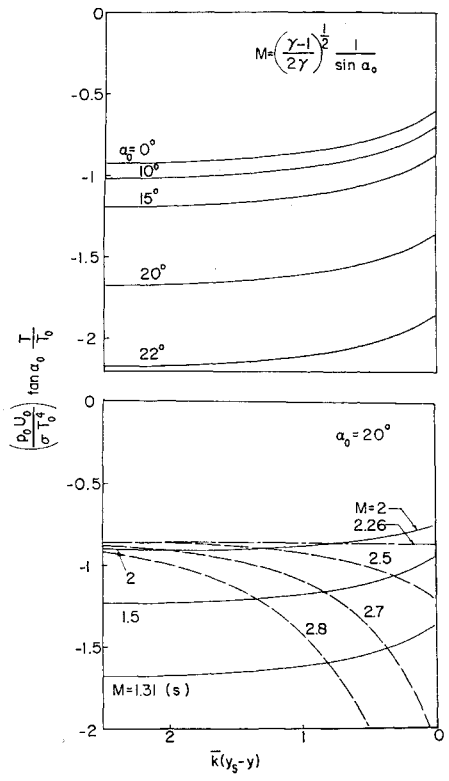

Fig. 12 The temperature perturbation across an oblique shock layer for various shock-layer angles α_0 and shock strengths in an optically thick, gray, perfect gas with $\gamma = 1.67$.

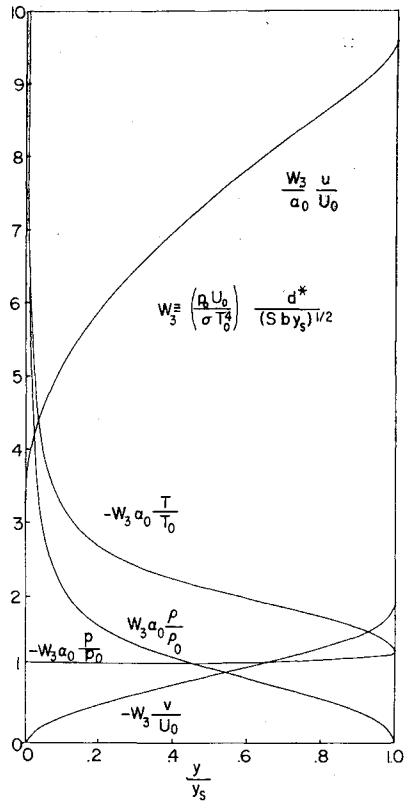

Fig. 13 The perturbations across an oblique shock layer in the limit of a strong shock and $\alpha_0 \to 0$ for a perfect ($\gamma = 1.67$) gas with a spectrum consisting of collision-broadened nonoverlapping lines.

wedge surface. At distances appreciably greater than $(4b/S)\cot\alpha_0$ from the wedge vertex, these "boundary layers" will be small compared to the shock-layer thickness. The perturbations u, ρ, and T are easily computed using the foregoing expression for p in Eqs. (39, 40, and 5). The expression for ρ involves the term

$$\frac{1}{U_0}\int_{y\cot\alpha_0}^{x}\epsilon\{\xi, y\}d\xi = \frac{4}{3}\left(\frac{z}{fk+z}\right)\left(\frac{\sigma T_0^4}{p_0 U_0}\right)\frac{(Sb)^{1/2}}{d^*}\times \left[\frac{(x\tan\alpha_0 - y)}{y^{1/2}} + 2(x\tan\alpha_0 - y)^{1/2}\right] \quad (66)$$

This term produces a large density and temperature perturbations at the surface because of the $y^{-1/2}$ term. The corresponding $\int\epsilon\{\xi, y\}d\xi$ term produced the large density and temperature perturbations near the surface in the optically thick, gray-gas case.

Considered as functions of the fractional distance across the shock layer y/y_s, the perturbations have similar profiles at different x stations with the magnitudes of the perturbations growing as $x^{1/2}$. The perturbations in the limit of a strong shock and $\alpha_0 \to 0$ are plotted in Fig. 13. The profiles resemble those for a transparent gas plotted in Fig. 6, but with the effects of absorption being evident, especially near the wedge surface and the shock front. The ρ and T perturbations shown to diverge as $y^{-1/2}$ at $y = 0$ because of the term given by Eq. (66) will straighten out in the "boundary layer" extending from $y = 0$ to about $y = 4b/S$ and will accordingly have finite values at $y = 0$. The perturbation pressure is seen to be nearly constant across the shock layer, although this result is not immediately obvious from the form of Eq. (64).

References

[1] Olfe, D. B., "The influence of radiant-energy transfer on one-dimensional shock wave propagation," *Supersonic Flow, Chemical Processes and Radiative Transfer*, edited by D. B. Olfe and V. Zakkay (Pergamon Press, Oxford, England, 1964), pp. 355–374.

[2] Zhigulev, V. N., Romishevskii, Y. A., and Vertushkin, V. K., "Role of radiation in modern gasdynamics," AIAA J. 1, 1473–1485 (1963).

[3] Goulard, R., "The coupling of radiation and convection in detached shock layers," J. Quant. Spectry. Radiative Transfer 1, 249–257 (1961).

[4] Kennet, H., "Radiation-convection interaction around a sphere in hypersonic flow," ARS J. **32**, 1616–1617 (1962).

[5] Yoshikawa, K. K. and Chapman, D. R., "Radiative heat transfer and absorption behind a hypersonic normal shock wave," NASA TN D-1424 (1962).

[6] Howe, J. F. and Viegas, J. R., "Solutions of the ionized radiation shock layer, including re-absorption and foreign species effects," NASA TR R-159 (1963).

[7] Wilson, K. H. and Hoshizaki, H., "Inviscid, nonadiabatic flow about blunt bodies," AIAA Preprint 64-70 (January 20–22, 1964).

[8] Griffith, W. C., "Interaction of a shock wave with a thermal boundary layer," J. Aeronaut. Sci. **23**, 16–23 (1956).

[9] Kourganoff, V., *Basic Methods in Transfer Problems* (Clarendon Press, Oxford, England, 1952).

[10] Penner, S. S., *Quantitative Molecular Spectroscopy and Gas Emissivities* (Addison-Wesley Publishing Co., Reading, Mass., 1959).

[11] Romishevskii, E. A., "The effect of radiation on the hypersonic flow past thin bodies," Inzh. Zh. **3**, 12–17 (1963); transl. as TT-10, School of Aeronautical and Engineering Sciences, Purdue Univ. (February 1964).

[12] Wang, K. C., "One-dimensional shock propagation with thermal radiation," Research Rept. RR-47, Martin Co., Baltimore, Md. (December 1963).